OXIDATION STATE OF CHASSIGNITES AND SHERGOTTITES FROM V-IN-OLIVINE OXYBAROMETRY. R. W. Nicklas[1], J. M. D. Day[1], A. Udry[2], Y. Liu[3], Z. Vaci[4] and K. T. Tait[5] [1]Scripps Institution of Oceanography, University of California, San Diego, La Jolla, CA 92093, USA. Email: rwnicklas@ucsd.edu, [2]Department of Geoscience, University of Nevada, Las Vegas, Las Vegas, NV 89154, USA, [3]Jet Propulsion Laboratory, California Institute of Technology, Pasadena, CA 91109, USA, [4]Institute of Meteoritics, Department of Earth and Planetary Science, University of New Mexico, Albuquerque, NM 87131, USA, [5]Royal Ontario Museum, Toronto, ON, M5S 2C6, Canada.

Introduction: The shergottite and chassignite meteorites originate from Mars, and have been used to constrain the composition of Mars and the evolution of its mantle and crust. Martian meteorites show a large range of isotopic signatures and incompatible trace element ratios indicating that they sample components that experienced differentiation early in Solar System history [1-3]. Two models exist that can explain these geochemical signatures: (1) mixing between a depleted mantle and ancient enriched crust [1] and (2) mixing between depleted and enriched mantle components established early in martian history [2]. Notably, the oxygen fugacity (fO_2) of shergottites has been suggested to correlate with degree of geochemical enrichment [1,2], implying that the enriched endmember is oxidized, although this has been disputed [3], Most published fO_2 measurements rely on near-solidus minerals like Fe-Ti oxides, or on the assumption of equilibrium between zoned grains of major phases. In this study, we measured fO_2 in a suite of high-MgO martian meteorites using the V-in-Olivine oxybarometer via Laser Ablation Inductively Coupled Plasma Mass Spectrometry (LA-ICP-MS), which relies on the empirically calibrated relationship between $D_V^{olivine/melt}$ and fO_2 [4]. As olivine is an early phase in primitive martian meteorites, this method measures melt fO_2 prior to any potential modification by late degassing or contamination.

Samples: Seven olivine-bearing martian meteorites were selected for study: the olivine-phyric shergottites Tissint, Larkman Nunataks (LAR) 12011 and Northwest Africa (NWA) 10416, the poikilitic shergottites NWA 10618 and NWA 12241, and the chassignites Chassigny and NWA 2737. The fO_2 of six samples have been previously reported: NWA 10618: ΔFMQ = -2.68±0.48 (poikilitic texture) [3] Tissint: ΔFMQ = -3.50 [5], LAR 12011 ΔFMQ = -2.7±1 [6], Chassigny ΔFMQ = -1.3 [7], NWA 2737 ΔFMQ = +0.6 [7] and NWA 10416 ΔFMQ = -3 (primitive value) [8]

Methods: Olivine grains within polished sections mounted in epoxy disks were analyzed with a *New Wave* UP-213 nm laser coupled to a *Thermo Scientific* iCAPq ICP-MS at the *Scripps Isotope Geochemistry Laboratory* (SIGL). The isotopes of interest were ^{25}Mg, ^{27}Al, ^{29}Si, ^{43}Ca, ^{45}Sc, ^{51}V, ^{57}Fe, ^{59}Co, ^{61}Ni, ^{71}Ga, ^{89}Y, ^{139}La, ^{140}Ce, ^{141}Pr, ^{146}Nd, ^{147}Sm, ^{153}Eu, ^{159}Tb, ^{160}Gd, ^{163}Dy, ^{165}Ho, ^{166}Er, ^{169}Tm, ^{172}Yb and ^{175}Lu. Each analysis consisted of ~20 seconds of background and ~40 seconds of ablation time. All ablation pits were 100 micron in diameter. Standards used in data reduction were BHVO-2g, BCR-2g, and BIR-1g. All data was corrected for ablation efficiency using ^{29}Si as an internal standard and data reduction was performed using an in-house reduction macro. Repeat analyses of the MongOL olivine standard [9] demonstrated that V concentration in olivine can be accurately measured using these parameters at a precision of 5% (2SD).

Results: At least 20 of the cores of texturally primitive olivine grains were analyzed in each meteorite, and following data reduction, the data were filtered to remove analyses potentially compromised by ablation of other phases such as spinel, pyroxene, or groundmass. This was done by examining the average Al content of each set of analyses, and removing any analyses enriched in Al beyond 2SD of the mean. As all phases in basaltic rocks are highly enriched in Al relative to olivine, this yields a much more consistent dataset for all elements. Vanadium concentration data in olivine for all of the studied meteorites are shown in *Figure 1*.

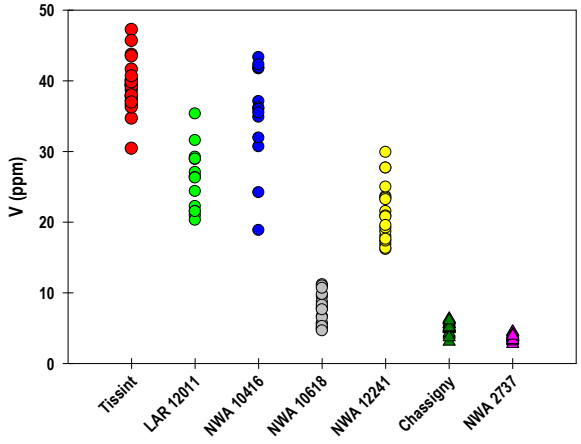

Figure 1: *Comparison of V concentrations in olivine from seven high-MgO martian meteorites. Shergottites are shown as circles, and chassignites are shown as triangles. Note lower concentrations and smaller variations in chassignites relative to shergottites.*

After filtering, the dataset for each meteorite consisted of analyses of at least 13 grains. The correlation between V abundance and Mg# is shown in *Figure 2*.

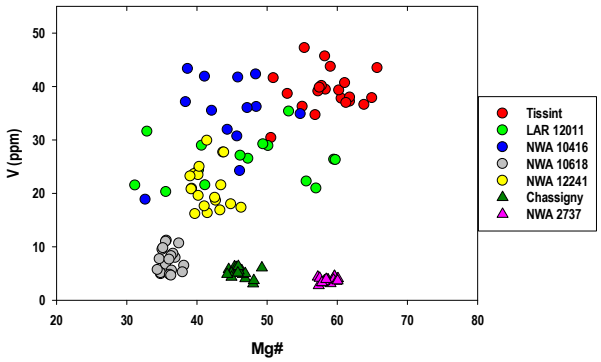

***Figure 2**: Mg# (Mg/(Mg+Fe)*100) plotted against V concentration for the studied olivine grains. Note the broad positive correlation of V with Mg# in shergottites. Chassignites plot off of this trend.*

As all the meteorites studied here have either lost or gained olivine via fractional crystallization, it is necessary to model the V concentration of melt in equilibrium with the analyzed olivines in order to constrain $D_V^{olivine/melt}$ and fO_2. Primitive lava MgO contents for each meteorite were gathered from literature sources [7, 10, 11]. Where unavailable, they were calculated using $K_D^{Fe\text{-}Mg} = 0.35$, and olivine major element data. Once the MgO content of the primary magma was known, the bulk rock V content [12] was adjusted by adding or subtracting the average olivine composition until the MgO content of the bulk was equal to that of the primary magma. In this way, primitive magma V content was constrained. Average olivine V content and primary magma V content of each meteorite were used to calculate $D_V^{olivine/melt}$ and then fO_2 using the experimental regression of [13]. No bulk rock V analysis of NWA 10618 exists, so fO_2 was not determined for that sample. Oxygen fugacity is shown plotted against La/Sm, a proxy for trace element enrichment in *Figure 3*.

Discussion: The dataset broadly supports the conclusions of [1] that degree of trace element enrichment positively correlates with primitive magma oxygen fugacity. Our new data agree with published data within errors for the shergottite samples, but are significantly more oxidized for chassignites. As olivine is the liquidus mineral and major phase in chassignites, our olivine oxybarometry is expected to yield the most primitive fO_2 value. The observation that trace element enrichment is correlated with fO_2 from the time that the meteorite parental melts cool to olivine saturation suggests that the observed correlation is a source signature and not the result of late contamination, in line with [2]. The high oxidation state of the chassignites supports the model of their formation from a recently metasomatized mantle source [12].

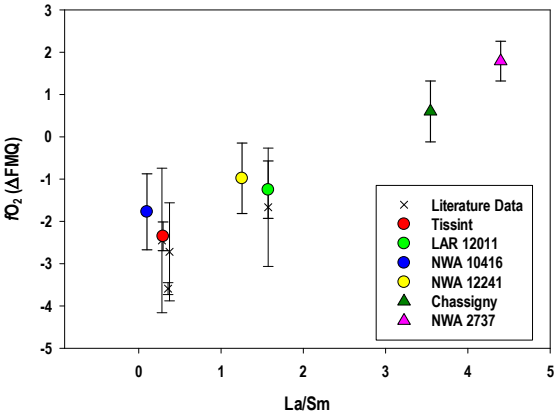

***Figure 3**: Calculated fO_2 values of martian meteorites using V-in-Ol as a function of La/Sm ratio. Literature values are calculated from published olivine and bulk rock data for the meteorites Y-980495, LAR 06319, LAR 12095, LAR 12240 using the same method described here.*

The V-in-Ol oxybarometer has been previously used to constrain the fO_2 of martian meteorites by [14], who concluded that primitive fO_2 correlates with degree of enrichment. The fO_2 ranges for depleted and enriched samples reported by [14] overlap with our data set, but no meteorites were analyzed by both studies. The technique used here shows promise for constraining the fO_2 of olivine-rich martian meteorites and demonstrates a fundamental difference in the oxidation state or primitive enriched and depleted mantle reservoirs on Mars. Comparison of this technique with those utilizing late-formed phases could also offer important constraints on the redox evolution of martian magmas

Funding: Support comes from the NASA Emerging Worlds program (JMDD).

References: [1] Herd C. D. K. et al. (2002) *GCA, 66,* 2025–2036. [2] Herd C. D. K. (2003) *MAPS, 38,* 1793-1805. [3] Rahib R. R. et al. (2019) *GCA, 266,* 463-496. [4] Nicklas R. W. et al. (2018) *GCA, 222,* 447–466. [5] Castle N., Herd C. D. K. (2017) *MAPS, 52,* 125-146. [6] Balta J. B. et al. (2013) *MAPS, 48,* 1359-1382. [7] Beck et al. (2006) *GCA, 70,* 2127-2139. [8] Herd C. D. K. et al (2016) *LPS XLVII* Abstract#2527. [9] Batanova (2019) *GGR, 43,* 453-473. [10] Johnson M. C. (1991) *GCA, 55,* 349-366. [11] Herd C. D. K. et al. (2013) *LPS XLIV* Abstract#2683 [12] Day J. M. D. et al. (2018) *Nat. Comm., 9,* 4799. [13] Wang J. (2019) *JGR Solid Earth, 124,* 4617-4638. [14] Shearer C. K. et al. (2006) *Am. Min. 91,* 1657-1663.